

Arylethynyl Derivatives of the Dihydroazulene/ Vinylheptafulvene Photo/Thermoswitch: Tuning the Switching Event

Søren Lindbæk Broman, Michael Åxman Petersen, Christian G. Tortzen,
Anders Kadziola, Kristine Kilså, and Mogens Brøndsted Nielsen*

Department of Chemistry, University of Copenhagen, Universitetsparken 5,
DK-2100 Copenhagen Ø, Denmark

Received April 23, 2010; E-mail: mbn@kiku.dk

Abstract: A selection of dihydroazulene (DHA) photoswitches incorporating an arylethynyl-substituent in the seven-membered ring was prepared by palladium-catalyzed Sonogashira cross-coupling reactions employing a suitable bromo-functionalized DHA. Shielding of the alkyne bridge and separating the aryl and DHA units, by sterically demanding groups, was required to obtain stable compounds. The DHAs underwent a light-induced ring-opening to vinylheptafulvenes (VHFs) which were thermally converted to a mixture of two DHA regioisomers, one of which was the original one. The influence of the aryl groups on the DHA and VHF absorptions and on their interconversion was investigated in detail. The rates of the switching events were finely tuned by the donor or acceptor strength of the aryl group. The thermal ring closure was found to proceed most readily in the presence of an electron-donating group on the seven-membered ring. The rate constant was found to follow a Hammett linear free energy correlation, which signals that stabilization of a positive charge in the seven-membered ring plays a crucial role in the ring-closure reaction. In view of these findings, it was possible to control the switching event by protonation/deprotonation of an anilino-substituted DHA. Also, the light-induced ring opening reaction was strongly controlled by acid/base. In addition to the mesomeric effects exerted by an arylethynyl group, the inductive effects exerted by different groups on the thermal ring closure were elucidated. Although the alkyne bridge transmits the electronic character of the aryl group, the ring-closure is retarded for all the ethynylated compounds relative to the parent unsubstituted compound. Along with our synthesis of suitable arylalkynes, we discovered an interesting byproduct in a Sonogashira cross-coupling reaction involving a nitrophenyl group, namely a diaryl azoxy compound. Its structure was confirmed by X-ray crystallographic analysis.

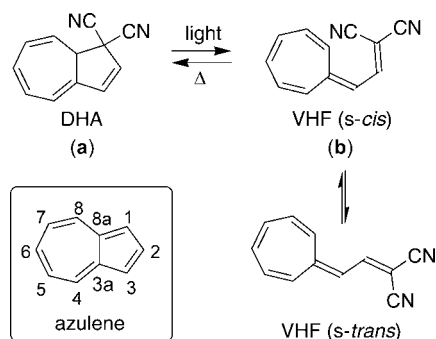
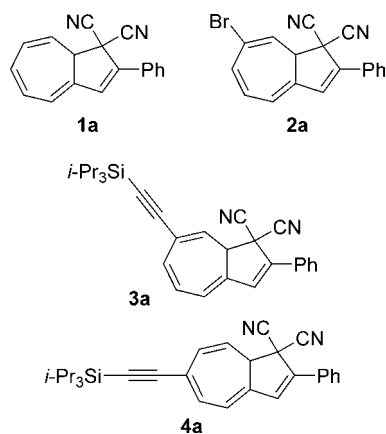
Introduction

Molecular switches possess at least two reversibly interconvertible molecular states and are important within the field of molecular electronics, photonic devices, and advanced molecular and supramolecular materials.¹ Particular attention has been paid

to photoswitches, such as azobenzenes and dithienylethenes, that can be interconverted between two states by light.² The term photochromism is used to characterize the properties of such compounds that change their optical absorption upon light-induced isomerization. Synthetic protocols are available for ready functionalization of both rings in azobenzenes and dithienylethene compounds with suitable groups, such as electron donor and acceptor units (push–pull photochromophores), anchoring groups for adhesion to electrodes, functional groups that provide liquid crystallinity, or groups for incorporation of the photoswitch into biological systems.² One photoswitch that has been less explored in advanced systems is the dihydroazulene/vinylheptafulvene (DHA/VHF) system incorporating two cyano groups at C-1 (Scheme 1).^{3,4} DHA undergoes a photochemically induced ring-opening to VHF, usually with a notably higher quantum yield than that of the *trans* to *cis* isomerization of azobenzenes. VHF in turn

- (1) (a) Balzani, V.; Gómez-López, M.; Stoddart, J. F. *Acc. Chem. Res.* **1998**, *31*, 405–414. (b) *Molecular Switches*; Feringa, B. L., Eds.; Wiley-VCH: Weinheim, Germany, 2001. (c) Weibel, N.; Grunder, S.; Mayor, M. *Org. Biomol. Chem.* **2007**, *5*, 2343–2353. (d) Berg, T. *Angew. Chem., Int. Ed.* **2009**, *48*, 3218–3220.
- (2) (a) Irie, M. *Chem. Rev.* **2000**, *100*, 1685–1716. (b) Kawata, S.; Kawata, Y. *Chem. Rev.* **2000**, *100*, 1777–1788. (c) Tian, H.; Yang, S. *J. Chem. Soc. Rev.* **2004**, *33*, 85–97. (d) Raymo, F. M.; Tomasulo, M. *Chem. Soc. Rev.* **2005**, *34*, 327–336. (e) Volgraf, M.; Gorostiza, P.; Numano, R.; Kramer, R. H.; Isacoff, E. Y.; Trauner, D. *Nat. Chem. Biol.* **2006**, *2*, 47–52. (f) Matharu, A. S.; Jeeva, S.; Ramanujam, P. S. *Chem. Soc. Rev.* **2007**, *36*, 1868–1880. (g) Whalley, A. C.; Steigerwald, M. L.; Guo, X.; Nuckolls, C. *J. Am. Chem. Soc.* **2007**, *129*, 12590–12591. (h) Yagai, S.; Kitamura, A. *Chem. Soc. Rev.* **2008**, *37*, 1520–1529. (i) Fortin, D. L.; Banghart, M. R.; Dunn, T. W.; Borges, K.; Wagenaar, D. A.; Gaudry, Q.; Karakossian, M. H.; Otis, T. S.; Kristan, W. B.; Trauner, D.; Kramer, R. H. *Nat. Methods* **2008**, *5*, 331–338. (j) Liang, X.; Mochizuki, T.; Asanuma, H. *Small* **2009**, *5*, 1761–1768. (k) Sadiwsi, O.; Beharry, A. A.; Zhang, F.; Woolley, G. A. *Angew. Chem., Int. Ed.* **2009**, *48*, 1484–1486. (l) Hoppmann, C.; Seedorff, S.; Richter, A.; Fabian, H.; Schmieder, P.; Rück-Braun, K.; Beyersmann, M. *Angew. Chem., Int. Ed.* **2009**, *48*, 6636–6639.

- (3) (a) Daub, J.; Knöchel, T.; Mannschreck, A. *Angew. Chem., Int. Ed. Engl.* **1984**, *23*, 960–961. (b) Daub, J.; Gierisch, S.; Klement, U.; Knöchel, T.; Maas, G.; Seitz, U. *Chem. Ber.* **1986**, *119*, 2631–2646. (c) Gierisch, S.; Daub, J. *Chem. Ber.* **1989**, *122*, 69–75. (d) Gierisch, S.; Bauer, W.; Burgemeister, T.; Daub, J. *Chem. Ber.* **1989**, *122*, 2341–2349. (e) Spritzer, H.; Daub, J. *Liebigs Ann.* **1995**, 1637–1641. (f) Spritzer, H.; Daub, J. *Chem.—Eur. J.* **1996**, *2*, 1150–1158.

Scheme 1. Dihydroazulene (DHA)–Vinylheptafulvene (VHF) Photoswitch**Chart 1.** Functionalized DHAs

undergoes a thermally induced ring-closure back to DHA. The initially formed *s-cis*-VHF is in equilibrium with the generally more stable *s-trans*-VHF. The large structural difference between the DHA and VHF isomers, both in regard to conjugation, spatial shape, and dipole moment,⁵ is reflected by significantly different absorption maxima of the two species. Thus, the phenyl-substituted DHA **1a** (Chart 1) exhibits an absorption maximum (λ_{max}) at 354 nm in MeCN, while the related VHF **1b** absorbs at $\lambda_{\text{max}} = 471$ nm.⁶ The letters **a** and **b** will be used in general to designate a pair of DHA (**a**) and VHF (**b**) compounds that are interconvertible. Another attractive property of the system is that both the light-induced DHA→VHF and the thermal VHF→DHA conversion proceeds quantitatively, while *cis*–*trans* isomerizations are often characterized by a photostationary equilibrium.

The pioneering work by Daub and co-workers³ has allowed ready incorporation of a variety of aryl groups in the five-membered ring of DHA. The aryl group is conveniently included early in the synthesis before the final DHA is formed. One major obstacle has been the incorporation of functional groups in the seven-membered ring of DHA. Indeed, we reckon that the lack of synthetic protocols for functionalizing both the five- and seven-membered rings is one of the main reasons why the DHA/

VHF system has been less explored in advanced systems. The conjugated part of DHA has seven possible positions (C2, C3, C4, C5, C6, C7, and C8; for numbering, see Scheme 1) at which its properties can be potentially tuned by substituent groups and at which it can be incorporated into larger systems. We have very recently taken the first step toward advancing the chemistry of the seven-membered ring.^{7,8} Thus, an efficient regioselective bromination–elimination protocol was devised for preparing the bromo-substituted DHA **2a** from DHA **1a** (Chart 1). Special care was required in the elimination step to avoid elimination of HCN along with HBr, which would furnish the corresponding 10 π -aromatic azulene. Indeed, the choice of base was rather delicate, but it was found that LiN(SiMe₃)₂ provided the desired elimination product **2a** in a yield of >90%.^{7b} Subsequently a Sonogashira cross-coupling reaction⁹ with triisopropylsilylacetylene provided the product **3a** that after a ring-opening/closure cycle provided a mixture of the two regioisomers **3a** and **4a**. The ratio was controlled by both the wavelength of irradiation and the solvent polarity (**3a**:**4a** ratio of 1:2 in MeCN and 1:0 in cyclohexane after one light (353 nm)–heat cycle). Here we present the further scope of compounds **2a** and **3a** for Sonogashira cross-coupling reactions with the aim to functionalize DHA with electron-donating and electron-withdrawing aryl groups. The ultimate goal was to determine to which extent the acetylenic spacer transmits the donor or acceptor property of the aryl group, which is expected to influence the switching event.

Results and Discussion

Our first objective was to subject compound **3a** to further acetylenic scaffolding. This required removal of the silyl protecting group to provide the terminal alkyne. First, desilylation of **3a** was attempted by a fluoride source (Bu₄NF) in wet THF. However, these conditions caused elimination of HCN to provide a mixture of azulenes. For this reason we decided to incorporate the more labile trimethylsilyl-protecting group by treating the bromide **2a** with trimethylsilylacetylene according to the conditions provided in Scheme 2. Careful treatment of the resulting DHA **5a** with Bu₄NF again resulted in elimination of HCN as did treatment with K₂CO₃ in a mixture of THF and MeOH. Yet, treating DHA **5a** with acetic acid before addition of the fluoride source gave, gratifyingly, the terminal alkyne **6a** in high yield. Next, this alkyne was treated with iodobenzene under Sonogashira cross-coupling conditions. We were able to isolate DHA **7a** from this reaction. A spot of the species on a TLC plate changed color from yellow to violet after exposure to UV light. Also, the ¹H NMR spectrum indicated formation of the right product. Yet, the compound was not stable in solution and degraded to an unidentified species that was no longer photochromic. A simple TLC inspection readily allows one to identify the presence or absence of a DHA species as the spot changes color from yellow to red or violet (depending

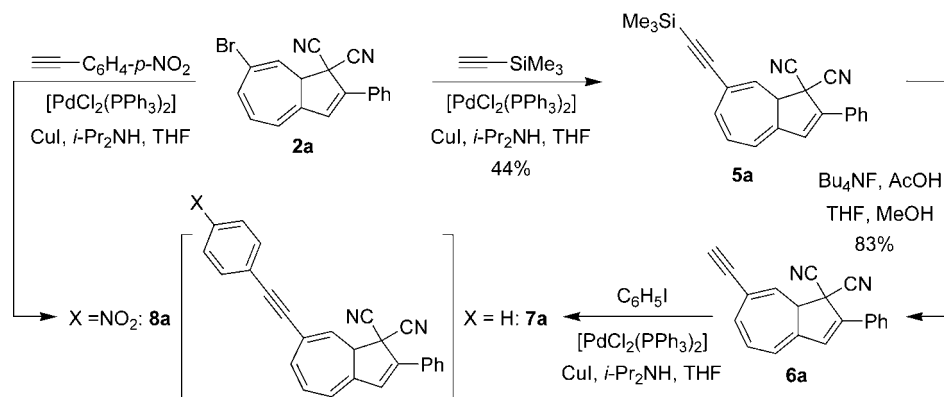
(4) (a) Gobbi, L.; Seiler, P.; Diederich, F. *Angew. Chem., Int. Ed.* **1999**, *38*, 674–678. (b) Petersen, M. Å.; Zhu, L.; Jensen, S. H.; Andersson, A. S.; Kadziola, A.; Kilså, K.; Nielsen, M. B. *Adv. Funct. Mater.* **2007**, *17*, 797–804. (c) Petersen, M. Å.; Andersson, A. S.; Kilså, K.; Nielsen, M. B. *Eur. J. Org. Chem.* **2009**, 1855–1858.
 (5) Plaquet, A.; Champagne, B.; Castet, F.; Ducasse, L.; Bogdan, E.; Rodriguez, V.; Pozzo, J.-L. *New J. Chem.* **2009**, *33*, 1349–1356.
 (6) Görner, H.; Fischer, C.; Gierisch, S.; Daub, J. *J. Phys. Chem.* **1993**, *97*, 4110–4117.

(7) (a) Petersen, M. Å.; Kilså, K.; Kadziola, A.; Nielsen, M. B. *Eur. J. Org. Chem.* **2007**, 1415–1418. (b) Petersen, M. Å.; Broman, S. L.; Kadziola, A.; Kilså, K.; Nielsen, M. B. *Eur. J. Org. Chem.* **2009**, 2733–2736.

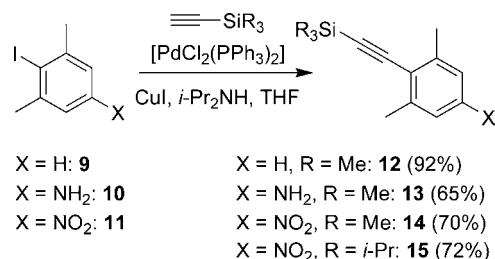
(8) We note that other DHA derivatives functionalized in the seven-membered ring are known, but these derivatives do not undergo light-induced conversion to VHF; see for example: (a) Prinzbach, H.; Herr, H.-J. *Angew. Chem., Int. Ed. Engl.* **1972**, *11*, 135–136. (b) Sugihara, Y.; Yamamoto, H.; Mizoue, K.; Murata, I. *Angew. Chem., Int. Ed. Engl.* **1987**, *26*, 1247–1249. (c) Yu, F.-F.; Yang, W.-G.; Shi, M. *Chem. Commun.* **2009**, 1392–1394.

(9) Sonogashira, K.; Tohda, Y.; Hagihara, N. *Tetrahedron Lett.* **1975**, 4467–4470.

Scheme 2. Synthesis of Arylethynyl-DHAs that Decomposed after Isolation



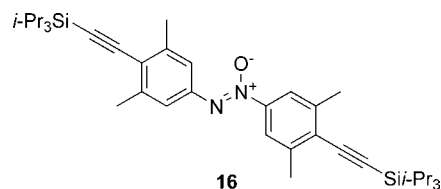
Scheme 3. Synthesis of Arylacetylenes with Methyl Groups Shielding the Alkyne



on the substitution) upon irradiation with UV-light within the region 350–400 nm. In another reaction, the bromide **2a** was subjected to a cross-coupling reaction with *p*-nitrophenylacetylene. Once again, we managed to isolate what seemed to be a DHA product (**8a**), but this compound as well underwent conversion to a yet unidentified non-DHA species.

Likely, the alkyne unit in **7a** and **8a** takes part in cycloaddition reactions. At the moment, it is unclear which product(s) are formed. No reaction was in fact observed by simply stirring parent compound **1a** and toluene in THF at 50 °C overnight (reflux in CH₂Cl₂ gave no conversion either). Moreover, alkyne **6a** could be isolated with no apparent decomposition. Despite these somewhat ambiguous results, we decided to shield the alkyne unit of the arylethynyl DHAs by bulky groups at the *ortho* positions on the phenyl ring. From the known iodides **9**,¹⁰ **10**,¹¹ and **11**,¹² the ethynylated aromatics **12**,¹³ **13**, **14**, and **15** were prepared (Scheme 3).

Interestingly, the cross-coupling conditions responsible for formation of **14** and **15** also provided a byproduct (10%) that in the latter case turned out to be the azoxybenzene **16** (Chart 2) as confirmed by X-ray crystallographic analysis (Figure 1).¹⁴ Thus, two molecules of **15** have been reductively dimerized. This is to our knowledge the first time such a species has been identified as a byproduct in the Sonogashira reaction of nitrobenzenes. However, an azoxy byproduct has been obtained previously in the presence of palladium; for example,

Chart 2. By-Product (Azoxy Compound) Formed from **15** under the Sonogashira Conditions

upon hydrogenation of nitrobenzene in the presence of [Pd(PhCN)₂Cl₂] in DMF.¹⁵ We have done some preliminary experiments to optimize the azoxy formation. First, formation of azoxybenzene was observed as well (according to GC–MS) by refluxing nitrobenzene, [PdCl₂(PPh₃)₂], and CuI in THF. The presence of CuI was required for any conversion to occur, while the presence of an amine was found to retard the reaction. Next, we subjected compound **15** to the conditions ([PdCl₂(PPh₃)₂] and CuI in THF, reflux), and found that 50 mol % of both

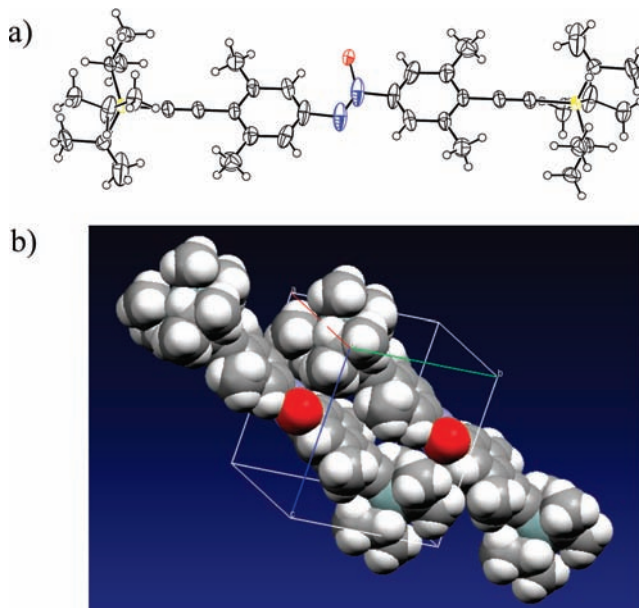
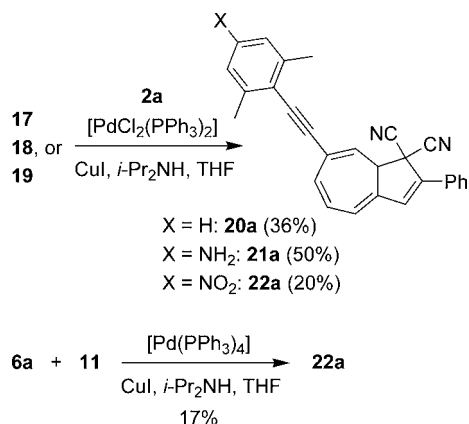


Figure 1. (a) X-ray crystal structure of the azoxy compound **16**. (b) The molecules are packed in layers dislocated in two dimensions (the figure was made with the program Mercury from the Cambridge Crystallographic Data Centre) and no π - π stacking is observed. The two phenyl moieties are virtually coplanar. Projected down the Si–Si line, the NO bond makes an angle of 18° with the remaining π -conjugated plane, presumably due to steric effects. The N–N and N–O distances are observed to be 1.24 and 1.49 Å, respectively.

- (10) Ohno, A.; Tsutsumi, A.; Yamazaki, N.; Okamura, M.; Mikata, Y.; Fujii, M. *Bull. Chem. Soc. Jpn.* **1996**, *69*, 1679–1685.
 (11) Kajigaeshi, S.; Kakinami, T.; Yamasaki, H.; Fujisaki, S.; Okamoto, T. *Bull. Chem. Soc. Jpn.* **1988**, *61*, 600–602.
 (12) (a) Bartoli, G.; Ciminale, F.; Todesco, P. E. *J. Org. Chem.* **1975**, *40*, 872–874. (b) Van Berk, P.; Van Langen, J. O. M.; Verkade, P. E.; Webster, B. M. *Recl. Trav. Pays-Bas* **1956**, *75*, 1137–1154. (c) Hodgson, H. H.; Walker, J. *J. Chem. Soc.* **1933**, 1620.
 (13) Saiki, T.; Akine, S.; Goto, K.; Tokitoh, N.; Kawashima, T.; Okazaki, R. *Bull. Chem. Soc. Jpn.* **2000**, *73*, 1893–1902.

Scheme 4. Synthesis of Stable Arylethynyl-DHAs



palladium and copper catalysts provided complete conversion to **16** (within 1 h as judged by TLC inspection).

The silyl protecting groups of **12–15** were removed under standard conditions, by either K_2CO_3 in MeOH/THF (removal of SiMe_3) or Bu_4NF in THF (removal of Si-Pr_3) to furnish alkynes **17**,¹⁶ **18**, and **19** in high yields.

The terminal arylalkynes were then subjected to palladium-catalyzed cross-coupling reactions with the DHA-bromide **2a** (Scheme 4). The resulting DHAs **20a**, **21a**, and **22a** were isolated in reasonable yields, and, gratifyingly, they were all resistant toward degradation upon standing in solution after isolation. Thus, our design strategy turned out successful; the two methyl groups are indeed able to shield the alkyne unit sufficiently to avoid degradation. Yet, we are not currently able to state whether the stabilizing effect is of steric or electronic character. Synthesis of the nitrophenyl-substituted DHA **22a** was the most difficult; it required ultrasound (using a sonication bath) to proceed. We have previously¹⁷ found ultrasound advantageous for the Sonogashira cross-coupling involving compounds that do not withstand prolonged heating. While compound **22a** is not stable under the Sonogashira conditions, it is perfectly stable when isolated pure. We found that microwave heating could also be employed for the reaction. DHA **22a** was also

(14) Compound **16** crystallizes in the triclinic crystal system, with the sum formula $\text{C}_{38}\text{H}_{58}\text{N}_2\text{O}\text{Si}_2$ and a unit cell volume of 934.5 \AA^3 . This means that there is only one molecule in the unit cell. Because the molecule itself does not possess an inversion center (the oxygen atom breaks the symmetry), the natural conclusion is that the space group must be $P1$. However, when solved in $P1$, peaks in the initial electron density map clearly display inversion symmetry. So albeit the space group must be $P1$, the molecule is disordered with the oxygen atom having two possible positions depending on the microscopic cell (a twin hypothesis was also tested but did not seem to be appropriate). On average, the space group cannot be distinguished from $P1$ and the structure refinement performs much better in this space group. First of all this description constrains all atoms with an inversion center and the oxygen population to 0.5. Second, the thermal ellipsoids appear more reasonable and the resulting difference Fourier reveals many of the hydrogen atoms which was not the case when attempted refined in $P1$.

(15) Mondal, T. K.; Banerjee, T. K.; Sen, D. *Indian J. Chem., Sect. A* **1980**, *19*, 846–848.

(16) Panda, J.; Virkler, P. R.; Detty, M. R. *J. Org. Chem.* **2003**, *68*, 1804–1809.

(17) (a) Qvortrup, K.; Andersson, A. S.; Mayer, J.-P.; Jepsen, A. S.; Nielsen, M. B. *Synlett* **2004**, 2818–2820. (b) Andersson, A. S.; Qvortrup, K.; Torbensen, E. R.; Mayer, J.-P.; Gisselbrecht, J.-P.; Boudon, C.; Gross, M.; Kadziola, A.; Kilså, K.; Nielsen, M. B. *Eur. J. Org. Chem.* **2005**, 3660–3671. (c) Andersson, A. S.; Kerndrup, L.; Madsen, A. Ø.; Kilså, K.; Nielsen, M. B.; La Porta, P. R.; Biaggio, I. *J. Org. Chem.* **2009**, *74*, 375–382.

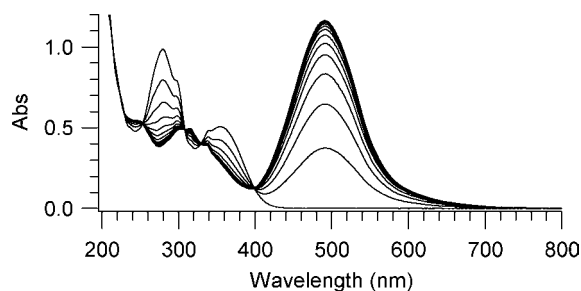


Figure 2. Irradiation of DHA **20a** ($1.2 \times 10^{-5} \text{ M}$) in MeCN with light (354 nm) during 0–140 s (10-s steps). The final VHF (**20b**) absorption spectrum is indicated by the thick curve.

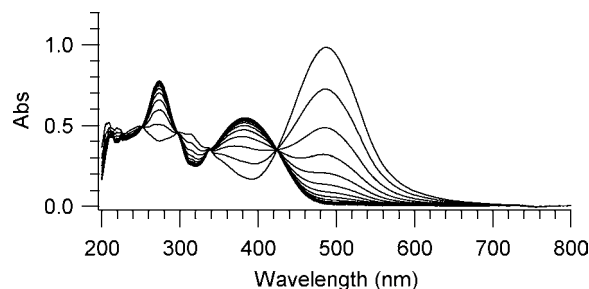


Figure 3. Thermal back-reaction of VHF **20b** ($1.2 \times 10^{-5} \text{ M}$) in MeCN monitored at $70 \text{ }^\circ\text{C}$ (2-min steps). The final DHA (**20a/26a**) absorption spectrum is indicated by the thick curve.

Chart 3. Terminal Alkynes

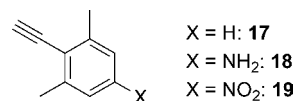


Chart 4. E/Z-VHFs

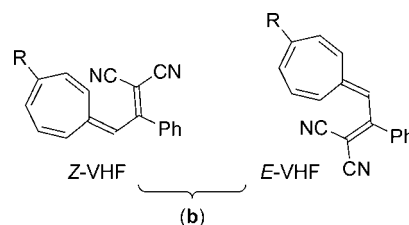
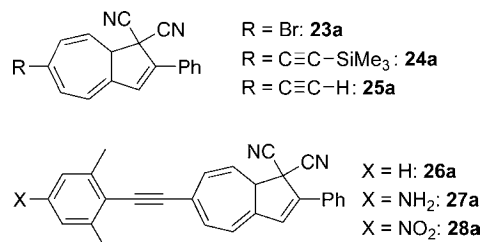


Chart 5. DHAs Substituted at Position 6



prepared by an alternative route, namely from the DHA–alkyne **6a** and the iodide **11** (Scheme 4). In effect, both DHAs **2a** and **6a** present useful building blocks for acetylenic scaffolding.

The selection of functionalized DHAs (designated by **a**) was subjected to switching studies in MeCN. They all underwent light-induced ring-opening to the corresponding VHF (**b**), which underwent thermal back-reactions. The absorption maximum of each individual DHA was used as excitation wavelength. The conversions are characterized by isosbestic points

Table 1. Absorption Maxima (λ_{max} /nm) of DHAs and VHF Measured in MeCN

substituent	7-substituted DHA	7-substituted/6-substituted DHA (ratio) ^a	6-substituted DHA ^b	E/Z-VHF
H	354 (1a)	—	—	471 (1b)
Br	356 (2a)	(7:3)	360 (23a)	461 (2b)
C≡C-Si-Pr ₃	355 (3a)	376 (1:2)	381 (4a)	476 (3b)
C≡C-SiMe ₃	355 (5a)	372 (5:7)	380 (24a)	476 (5b)
C≡C-H	355 (6a)	369 (7:4)	379 (25a)	469 (6b)
C≡C-Ar-H	354 (20a)	385 (1:1)	400 (26a)	490 (20b)
C≡C-Ar-NH ₂	330, 350 (sh ^c) (21a)	330/420 ^d	ca. 420 ^d (27a)	527 ^c (21b)
C≡C-Ar-NO ₂	344 (22a)	407 (5:3)	411 (28a)	482 (22b)

^a After one light–heat (ring-opening/closure) cycle, starting from the neat 7-substituted isomer; the ratios were calculated from the ¹H NMR spectra.

^b Absorption maximum was calculated by subtracting the absorption spectrum of the neat 7-substituted DHA from the absorption spectrum of the mixture using the isomer ratio obtained from ¹H NMR spectroscopy. ^c Sh = shoulder. ^d See text.

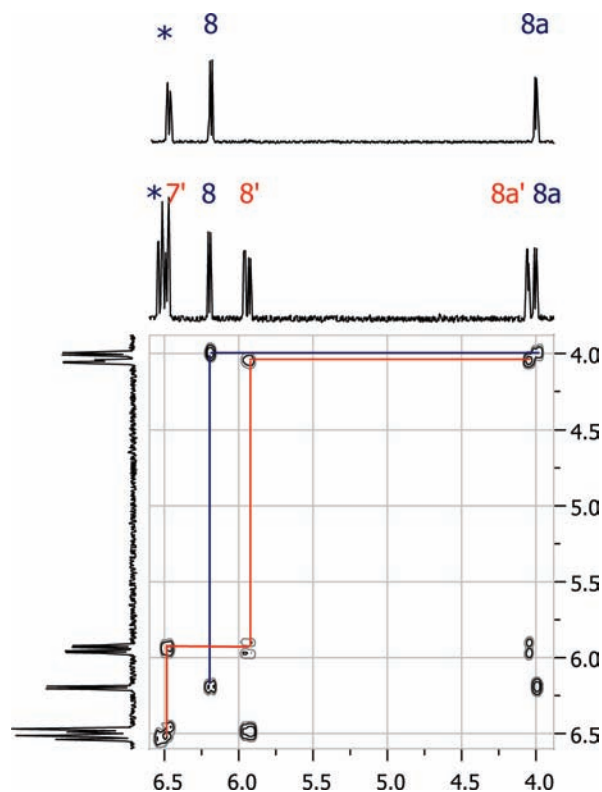


Figure 4. ¹H NMR Spectrum (CD₃CN) of **20a** and the COSY spectrum after one light–heat cycle, after which a mixture of **20a** and **26a** was formed. For the proton labeling, see Scheme 1. The numbers in blue refer to **20a**, while the primed numbers in red refer to **26a**. The symbol * indicates a signal that originates from either H-4, H-5, or H-6.

in the UV–vis absorption spectra. The change in the UV–vis absorption spectra for the light-induced opening of **20a** to **20b** is shown in Figure 2, while the thermal ring-closure of **20b** is shown in Figure 3. As observed previously,^{7b} the ring-opening reaction provided VHF *E/Z*-isomers (configuration of fulvene double bond; for simplicity, both VHF isomers are designated by the symbol **b**, Chart 4), while the thermal ring-closure reaction gave a mixture of 7- and 6-substituted DHAs (**23a–28a**, Chart 5). The ratio of *E* and *Z* isomers could be determined by ¹H NMR spectroscopy for the VHF **3b**, **5b**, **6b**, **20b**, and **22b** (by virtue of nonoverlapping signals for at least one group, allowing for determination of the integral ratio) and were in all cases ca. 1:1. The two DHA isomers are more readily distinguished by ¹H NMR spectroscopy, and a COSY spectrum supported the assignment of the new DHA species to the 6-substituted isomer. The COSY spectrum of **20a/26a** is shown in Figure 4. Coupling between protons H-8a and H-8 are seen for **20a**, but as expected no further coupling is seen for H-8. A

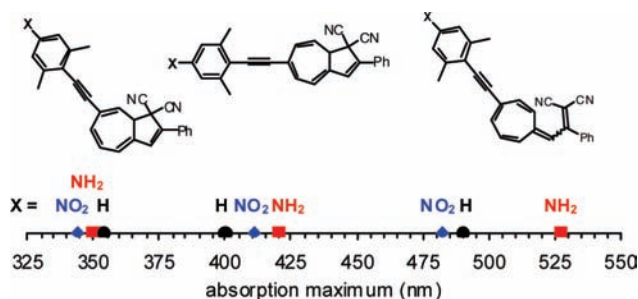


Figure 5. Summary of absorption maxima for the aryl-substituted DHAs and VHF. The shoulder at ca. 350 nm was plotted for **21a**.

new cross-peak is seen for **26a**, namely between protons H-8 and H-7, which signals that the substituent group is no longer placed at H-7 but at H-6. Moreover, the H-7 proton shows no further coupling. All of the three arylolethynyl-DHAs are stable up to at least 70 °C in nondegassed solution, and no bleaching was observed after five repetitive light–heat cycles (DHA → VHF → DHA).

A summary of absorption maxima for the compounds in MeCN in comparison to those previously studied (**1a,b**⁶ and **3a,b/4a**^{7b}) is provided in Table 1 together with DHA isomer ratios obtained after one light–heat cycle (the ratios did not change, however, after more cycles). Absorption maxima for the aryl-substituted derivatives are also summarized in Figure 5. First, we note that the 6-substituted DHA isomers exhibit significantly red-shifted absorption maxima relative to those of the 7-substituted ones; the absorption maxima of the 6-substituted DHAs were estimated from the maxima of the isomeric mixtures and the neat spectra of 7-substituted DHAs (by subtracting the spectra, employing the isomer ratios determined by NMR). These redshifts are explained by the fact that DHA takes a boat-like conformation,^{7b} and placement of the substituent group at position 6 instead of position 7 renders it part of a larger planar π -system comprised of C2–C6 and the phenyl group. The more efficient conjugation between DHA and the substituent when placed in position 6 is clearly realized by looking at the geometry-optimized structures of DHAs **20a** and **26a** (B3LYP/6-31G(d) level) obtained using the Gaussian 03 program package¹⁸ (Figure 6). The different absorption characteristics is most evident for the donor-substituted compounds **21a** and **27a**. This is not surprising, inasmuch as the transition likely has charge-transfer character. It was not possible to convert **21a** quantitatively to **21b** in MeCN (low quantum yield, *vide infra*). However, changing the solvent to cyclohexane allowed quantitative ring-opening. Transferring the resulting

(18) Frisch, M. J.; et al. *Gaussian 03, Revision B.03*; Gaussian, Inc.: Wallingford, CT, 2004.

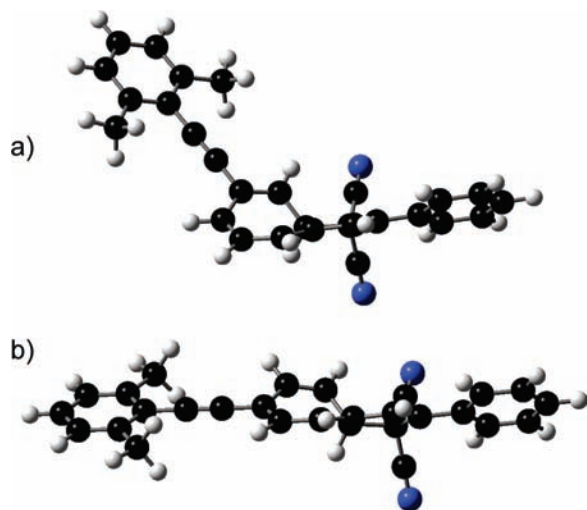


Figure 6. Geometry-optimized structures of (a) **20a** and (b) **26a**. Calculations were performed at the B3LYP/6-31G(d) level.

VHF **21b** (after removal of the solvent in vacuo) to MeCN, followed by thermal ring-closure to **21a** and **27a**, allowed estimation of the absorption maximum of **27a**. The value was in agreement with the one obtained by another experiment performed in MeCN, namely a cycle involving (i) protonation of **21a**, (ii) quantitative ring-opening, (iii) deprotonation, and (iv) ring-closure to **21a/27a** (*vide infra*). Significant tuning of the VHF absorption by virtue of the aryl group is also observed. Thus, the *p*-anilino derivative **21b** exhibits a considerably redshifted absorption maximum relative to that of the parent VHF **1b**, which is again explained by a charge-transfer character of the transition. The change is accompanied by a visible color change from red (**1b**) to violet (**21b**).

Rate constants (k) for the thermal back-reaction were measured at different temperatures (T) for each VHF. From Arrhenius plots, the activation energy E_a and pre-exponential factor A were obtained. A summary of kinetic data is provided in Table 2. First, we note that direct attachment of the electron-withdrawing bromo-substituent in compound **2b** results in a very slow ring-closure characterized by the longest half-life ($t_{1/2}$) in the series. Introducing an alkyne unit (**6b**) also retards the ring-closure in comparison to the parent compound **1b**. Comparison of the ethynylated compounds **3b**, **5b**, and **6b** reveals the effect of changing a trialkylsilyl for a hydrogen substituent: Inductive electron-donation by the silyl group enhances the rate of ring-closure. For the arylated compounds the rate constant depends on the donor- and acceptor-substitution at the *para* position of the aryl group. In fact, the data nicely fit a linear free energy correlation¹⁹ as revealed in Figure 7 in which $\ln k$ (25 °C) is plotted against the Hammett constant σ_p^+ (that includes *through-*

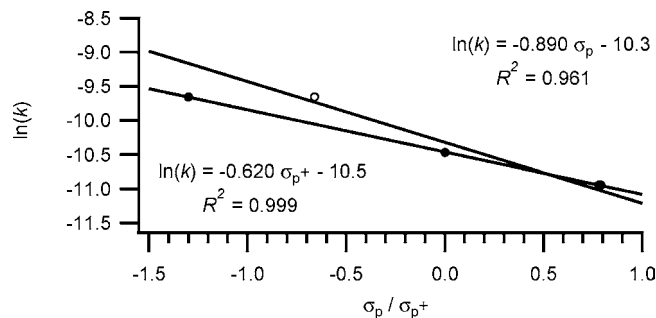


Figure 7. Linear free energy correlation between $\ln(k^{25\text{ °C}})$ and Hammett constants σ_p (○) and σ_p^+ (●). $\sigma_p(\text{NH}_2) = -0.66$, $\sigma_p(\text{H}) = 0$, $\sigma_p(\text{NO}_2) = 0.78$; $\sigma_p^+(\text{NH}_2) = -1.30$, $\sigma_p^+(\text{H}) = 0$, $\sigma_p^+(\text{NO}_2) = 0.79$. The points corresponding to H and NO_2 are overlapping.

conjugation; NH_2 : -1.30 , H : 0 , NO_2 : 0.79).²⁰ A straight line with a negative slope is obtained, which indicates that the ring-closure is enhanced by the ability of electron-donating substituents to stabilize a polar, zwitterionic transition state structure (Figure 8). This polar structure of the transition state structure was previously suggested by Daub^{3c} based on the fact that the ring-closure occurs faster in polar solvents and when an electron-withdrawing substituent is present on the five-membered ring.^{3c,6} Here we have unequivocally shown that an electron-withdrawing (EW) group in the heptafulvene ring slows the ring-closure, while an electron-donating (ED) one accelerate the ring-closure. Plotting $\ln k$ against the Hammett constant σ_p (NH_2 : -0.66 , H : 0 , NO_2 : 0.78)²¹ provides a poorer linear correlation than the one against σ_p^+ (Figure 7), which signals the importance of through-conjugation as depicted in Figure 8. It should be emphasized that while the effect of the aryl group is obviously transmitted via the alkyne bridge, the inherent property of the alkyne unit is to slow down the ring-closure, and this effect is not even overcome by an electron-donating anilino group as revealed by comparing **21b** and **1b**. Finally, we would like to stress the high stability of the arylethynyl-substituted DHAs/VHFs; no apparent decomposition occurs after five light-heat cycles as judged from the UV-vis absorption spectra.

The strong dependence on the character of the aryl substituent suggests that it should be possible to tune both the optical properties and the switching event by protonation/deprotonation of the anilino group in **21a**. As a matter of fact, protonation of the neutral DHA and VHF species results in significantly altered absorption properties as shown in Figure 9. As expected, the absorption of VHF **21b** is significantly blueshifted from λ_{max} 527 nm to λ_{max} 492 upon protonation. In addition, ring-closure of the protonated VHF is hampered as the rate constant is lowered by a factor of ca. 2, and the Arrhenius plot coincides with that of **20b** (cf., Supporting Information S38). The different ring-closure rate of neutral **21b** and protonated **21b** (**21b**· H^+)

Table 2. Kinetic Data for the Thermal Ring-Closure of *E/Z*-VHFs

substituent	<i>E/Z</i> -VHF	E_a (kJ/mol)	A (s^{-1})	$t_{1/2}^{50\text{ °C}}$ (min)	$t_{1/2}^{25\text{ °C}}$ (min)	$k^{25\text{ °C}}$ (s^{-1})
H	1b ^a	84.9	4.7×10^{11}	—	165	7.0×10^{-5}
Br	2b	93.7 ± 0.4	2.3×10^{11}	49.0	909	1.27×10^{-5}
$\text{C}\equiv\text{C}-\text{Si}i\text{-Pr}_3$	3b ^b	93.8 ± 0.5	3.0×10^{10}	35.0	670	1.7×10^{-5}
$\text{C}\equiv\text{C}-\text{SiMe}_3$	5b	94.6 ± 0.6	6.4×10^{11}	33.9	658	1.76×10^{-5}
$\text{C}\equiv\text{C}-\text{H}$	6b	94.2 ± 0.6	4.1×10^{11}	46.8	893	1.29×10^{-5}
$\text{C}\equiv\text{C}-\text{Ar}-\text{H}$	20b	91.4 ± 0.8	2.9×10^{11}	23.2	407	2.84×10^{-5}
$\text{C}\equiv\text{C}-\text{Ar}-\text{NH}_2$	21b	90.4 ± 0.7	4.5×10^{11}	10.4	182	6.42×10^{-5}
$\text{C}\equiv\text{C}-\text{Ar}-\text{NO}_2$	22b	93.7 ± 0.7	4.6×10^{11}	34.7	654	1.76×10^{-5}

^a Reference 6. ^b Reference 7b.

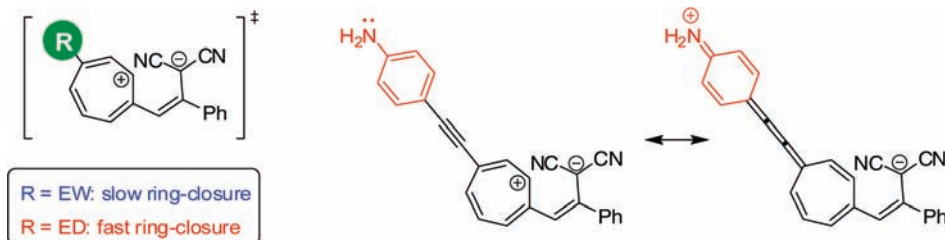


Figure 8. Ring-closure of VHF is strongly controlled by the electronic properties of the substituent, which implies the involvement of a zwitterionic structure for the transition state. An electron-donating (ED) *p*-anilino group will exert a through-conjugation stabilizing effect on the transition state.

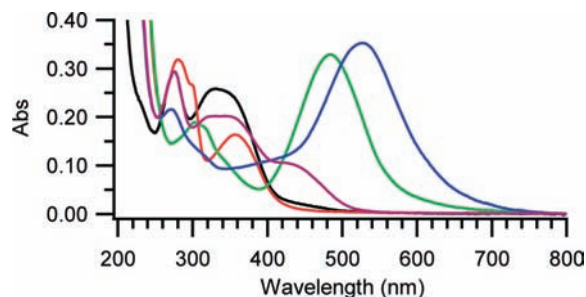


Figure 9. Changes in absorption spectra upon protonation of **21a** (black) and **21b** (blue) in MeCN. Protonation of **21a** causes a small redshift (red) and of **21b** a blueshift (green). Thermal ring-closure of **21b** results in a mixture of **21a** and **27a** (purple).

offers the possibility to control the switching event by acid/base. Thus, irradiation with light (330 nm) cannot fully convert DHA **21a** to VHF **21b**, but upon protonation (large excess of trifluoroacetic acid or 1 mol equiv of *p*-toluenesulfonic acid), DHA **21a**•H⁺ is fully converted to VHF **21b**•H⁺ after 1 min of irradiation (356 nm). Upon addition of NEt₃, (large excess), the neutral VHF **21b** is obtained. A test experiment showed that the ring-closure of **20b** was not affected by the presence of acid. Quantum yields for the light-induced ring-opening of **21a** and of the protonated species hereof were measured at an excitation wavelength of 355 nm relative to that of the parent DHA **1a** for which $\phi_{\text{DHA-VHF}} = 0.55$.⁶ Thus, experiments were performed under similar conditions (same lamp, time of irradiation, excitation wavelength and absorbance at this wavelength). For **21a** we obtain in this way a quantum yield of only 1.4%, while protonation increases the quantum yield of ring-opening to 60% for **21a**•H⁺. The results are summarized in Figure 10.

Conclusions

In conclusion, novel DHA derivatives functionalized with an arylolefinyl in the seven-membered ring were successfully prepared. The synthesis, however, required shielding of the alkyne unit by two methyl groups at the *ortho* positions of the aryl. These compounds are stable in solution in contrast to those without the two methyl groups, and they were subjected to both light-induced ring-opening and thermal ring-closure reactions. The synthesis takes advantage of our bromination–elimina-

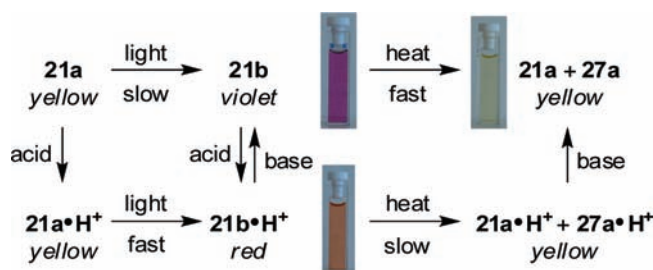


Figure 10. Control of the switching events by acid/base. The terms fast and slow refer to the same switching event, either ring-opening or ring-closure.

tion–cross-coupling strategy for directly functionalizing DHA regioselectively on the seven-membered ring. The donor or acceptor character of the aryl group is transmitted through the alkyne bridge. Thus, studies on the thermal ring-closure of the corresponding VHF compounds provide a Hammett linear free energy relationship. The slope of the Hammett plot indicates a zwitterionic structure of the transition state. In accordance with this picture, inductive electron withdrawal was found to hamper the ring-closure; in fact, a bromo-substituted VHF exhibited the slowest back-reaction among the compounds investigated. The quantum yield for the ring-opening was significantly decreased for the *p*-anilino-substituted DHA relative to the parent DHA **1a**. Yet, upon protonation of the NH₂ group, a similar quantum yield as that of **1a** was obtained. The opposing effects exerted by donor and acceptor groups were employed in a pH-controlled switch based on this *p*-anilino-substituted DHA. In addition, protonation resulted in significantly changed absorption properties of both the DHA and VHF species. In particular, the VHF absorption maximum is strongly altered by the functional group in the heptafulvene ring. The different absorption properties of 6- and 7-substituted DHAs, reflecting different degrees of conjugation efficiencies, also deserve mention. Altogether, the different absorption profiles make the system particularly attractive for advanced, photochromic materials.

In parallel work, we are exploring the possibility of using the DHA-bromide for other metal-catalyzed cross-coupling reactions. We reckon that direct attachment of the aryl donor/acceptor group on the seven-membered ring will influence the VHF ring-closure more strongly. Thus, while an alkyne bridge does transmit the electron-donating or -attracting character of the aryl group, it also hampers the ring-closure event. Moreover, functionalization at the remaining positions on the seven-membered ring of DHA may allow for further fine-tuning of the switching event in the future. We are currently working on

- (19) For examples of other photo/thermoswitches, for which Hammett correlations were established, see: (a) Swansburg, S.; Buncel, E.; Lemieux, R. *J. Am. Chem. Soc.* **2000**, *122*, 6594–6600. (b) Lu, N. T.; Nguyen, V. N.; Kumar, S.; McCurdy, A. *J. Org. Chem.* **2005**, *70*, 9067–9070. (c) Cordes, T.; Schadendorf, T.; Priewisch, B.; Rück-Braun, K.; Zinth, W. *J. Phys. Chem. A* **2008**, *112*, 581–588.
 (20) Brown, H. C.; Okamoto, Y. *J. Am. Chem. Soc.* **1958**, *80*, 4979–4987.
 (21) McDaniel, D. H.; Brown, H. C. *J. Org. Chem.* **1958**, *23*, 420–427.

the development of other synthetic protocols for obtaining these remaining regioisomers.

Experimental Section

General Methods. All solvents used for Sonogashira cross-coupling reactions were thoroughly degassed at a sonication bath with argon bubbling through. NMR Spectra were measured on 300 or 500 MHz instruments. All chemical shift values in the ^1H - and ^{13}C NMR spectra are referenced to the solvent ($\delta_{\text{H}} = 7.26$ ppm, $\delta_{\text{C}} = 77.26$ ppm). Coupling constants 3J and 4J refer to proton–proton 3-bond and 4-bond couplings, respectively. Thin Layer Chromatography (TLC) was carried out on commercially available pre-coated plates (silica 60) with fluorescence indicator; color change of the spot from yellow to red or in some cases violet upon irradiation by UV-light indicated the presence of a DHA. For column chromatographic purification of DHAs, the column was covered by an alumina foil to exclude light; the isolated fractions were also kept in the dark. All melting points are uncorrected. All spectroscopic measurements (including photolysis) were performed in a 1-cm path length cuvette. UV–vis absorption spectra were obtained by scanning the wavelength from 800 to 200 nm. Photoswitching experiments were performed using a 150 W xenon arc lamp equipped with a monochromator; the DHA absorption maximum for each individual species was chosen as the wavelength of irradiation (line width ± 2.5 nm). The thermal ring-closure was performed by heating the sample (cuvette) by a Peltier unit in the UV–vis spectrophotometer. Light – heat cycles described above correspond to the following two steps: *i*) irradiation of the DHA species until no further changes in the absorption spectrum were observed, *ii*) heating of the formed VHF species until no further changes in the absorption spectrum were observed.

7-Bromo-2-phenyl-1,8a-dihydroazulene-1,1-dicarbonitrile (2a)—**General Procedure.** Freshly prepared 7,8-dibromo-2-phenyl-1,7,8,8a-tetrahydroazulene-1,1-dicarbonitrile (according to literature protocol^{7a}) (416 mg, 1.00 mmol) was dissolved in dry THF (20 mL) at 0 °C. A solution of LiHMDS (1.10 mL, 1.10 mmol, 1 M) in toluene was added and the solution was stirred for 2 h while the temperature was allowed to rise to rt. The solution was diluted with Et₂O (100 mL) and washed with saturated aqueous NH₄Cl (2 × 100 mL). The organic phase was dried with MgSO₄, filtered, and the solvent evaporated in vacuo. The crude product can be employed directly for palladium-catalyzed cross-coupling reactions. An analytically pure sample was obtained (with loss of product) by column chromatography (SiO₂, 30% Et₂O/heptanes) followed by recrystallization from CH₂Cl₂/heptanes (1:10 v/v). ^1H NMR (300 MHz, CDCl₃): $\delta = 7.74$ (m, 2 H), 7.48 (m, 3 H), 6.89 (s, 1 H), 6.53 (m, 2 H), 6.31 (m, 1 H), 6.13 (d, $^3J = 4.4$ Hz, 1 H), 3.80 (dd, $^3J = 4.4$ Hz, $^4J = 1.7$ Hz, 1 H) ppm. ^{13}C NMR (75 MHz, CDCl₃): $\delta = 141.9$, 141.2, 132.9, 132.3, 131.8, 130.7, 130.1, 129.5, 126.6, 120.3, 120.2, 120.0, 114.8, 112.6, 51.2, 44.8 ppm. HR-MS: $m/z = 357.0003$ [MNa⁺]; calcd for C₁₈H₁₁N₂BrNa: $m/z = 357.0003$.

2-Phenyl-7-(trimethylsilylethynyl)-1,8a-dihydroazulene-1,1-dicarbonitrile (5a). A crude batch of **2a** synthesized from 7,8-dibromo-2-phenyl-1,7,8,8a-tetrahydroazulene-1,1-dicarbonitrile (416 mg, 1.00 mmol), was dissolved in dry THF (10 mL). Diisopropylamine (0.5 mL), CuI (3.8 mg, 0.02 mmol), and [PdCl₂(PPh₃)₂] (70 mg, 0.10 mmol) were added and the solution was degassed by sonication for 10 min under an argon atmosphere. Trimethylsilylacetylene (0.3 mL, 2.1 mmol) was added, and the reaction mixture was stirred at 35–40 °C overnight. The solution was diluted with Et₂O (100 mL) and washed with saturated aqueous NH₄Cl (2 × 100 mL). The organic phase was dried with MgSO₄, filtered, and the solvent evaporated in vacuo. Purification by column chromatography (SiO₂, toluene, $R_f = 0.70$) yielded **5a** (156 mg, 44%) as a yellow to green solid. Mp 134.0–135.0 °C. ^1H NMR (300 MHz, CDCl₃): $\delta = 7.72$ –7.75 (m, 2 H), 7.52–7.44 (m, 3 H), 6.87 (s, 1 H), 6.51–6.63 (m, 2 H), 6.29 (d, $^3J = 5.9$ Hz, 1 H), 6.18 (d, $^3J = 4.7$ Hz, 1 H), 3.79 (dd, $^3J = 4.7$ Hz, $^4J = 1.7$ Hz, 1 H), 0.21 (s, 9 H) ppm. ^{13}C NMR (125 MHz, CDCl₃): $\delta = 141.4$, 140.3, 132.4,

131.8, 131.6, 130.5, 130.4, 129.5, 126.6, 125.4, 123.0, 120.7, 115.0, 112.8, 103.2, 94.9, 51.1, 45.0, 0.1 ppm. Calcd for C₂₃H₂₀N₂Si (352.5): C 78.37, H 5.72, N 7.95; found: C 78.17, H 5.74, N 7.90%. MS (ESP+): $m/z = 353.3$ [MH⁺].

7-Ethynyl-2-phenyl-1,8a-dihydroazulene-1,1-dicarbonitrile (6a).

The TMS-protected acetylene, **5a** (190 mg, 0.54 mmol), was dissolved in THF (20 mL). MeOH (20 mL), acetic acid (8.0 mL), and a solution of tetrabutylammonium fluoride (24.0 mL, 24.0 mmol, 1 M) in THF were successively added. The mixture was stirred at rt overnight. The solution was diluted with Et₂O (50 mL) and washed with saturated aqueous NH₄Cl (2 × 50 mL). The organic phase was dried with MgSO₄, filtered, and the solvent evaporated in vacuo. Purification by column chromatography (SiO₂, toluene, $R_f = 0.61$) yielded **6a** (126 mg, 83%) as a yellow to red solid. Mp 111–113 °C. ^1H NMR (500 MHz, CDCl₃): $\delta = 7.71$ –7.76 (m, 2H), 7.41–7.51 (m, 3 H), 6.87 (s, 1 H), 6.61 (dd, $^3J = 11.4$ Hz, $^3J = 6.2$ Hz, 1 H), 6.50 (d, $^3J = 11.4$ Hz, 1 H), 6.30 (d, $^3J = 6.2$ Hz, 1 H), 6.21 (d, $^3J = 4.6$ Hz, 1 H), 3.81 (dd, $^3J = 4.6$ Hz, $^4J = 1.4$ Hz, 1 H), 2.94 (s, 1 H) ppm. ^{13}C NMR (125 MHz, CDCl₃): $\delta = 141.5$, 140.3, 132.0, 131.9, 131.8, 130.6, 130.4, 129.6, 126.6, 126.0, 122.1, 120.7, 115.0, 112.7, 82.3, 51.0, 45.1 ppm; one signal missing.

3,5-Dimethyl-4-(trimethylsilylethynyl)aniline (13). The iodoaniline **10** (3.46 g, 14.0 mmol), was dissolved in dry, degassed THF (75 mL) under an argon atmosphere. Diisopropylamine (6.0 mL), CuI (26 mg, 0.14 mmol), and [PdCl₂(PPh₃)₂] (490 mg, 0.70 mmol) were added, and the solution was degassed by sonication under argon atmosphere for 20 min. Then trimethylsilylacetylene (6.0 mL, 42 mmol) was added, and the mixture was stirred at 40 °C for 2 days. The solution was diluted with Et₂O (200 mL) and washed with saturated aqueous NH₄Cl (2 × 150 mL). The organic phase was dried with MgSO₄, filtered, and the solvent evaporated in vacuo. Purification by column chromatography (SiO₂, CH₂Cl₂/hexanes 7:3 v/v, $R_f = 0.33$) yielded **13** (2.25 g, 65%) as a brownish oil. ^1H NMR (300 MHz, CDCl₃): $\delta = 6.33$ (s, 2 H), 3.68 (br s, 2 H), 2.38 (s, 6 H), 0.30 (s, 9 H) ppm. ^{13}C NMR (75 MHz, CDCl₃): $\delta = 146.4$, 142.3, 113.4, 112.9, 104.0, 100.0, 21.2, 0.5 ppm. HR-MS (ESP+): $m/z = 240.1188$ [MNa⁺]; calcd for C₁₃H₁₉NSiNa: $m/z = 240.1184$.

3,5-Dimethyl-4-(trimethylsilylethynyl)nitrobenzene (14). The idonitrobenzene **11** (3.84 g, 13.9 mmol), was dissolved in dry, degassed THF (35 mL) under an argon atmosphere. Diisopropylamine (2.5 mL), CuI (25 mg, 0.13 mmol), and [PdCl₂(PPh₃)₂] (240 mg, 0.34 mmol) were added and the solution was degassed by sonication for 10 min under argon. Then trimethylsilylacetylene (4.2 mL, 30 mmol) was added, and the mixture was stirred at 40 °C overnight. The solution was diluted with Et₂O (200 mL) and washed with saturated aqueous NH₄Cl (2 × 150 mL). The organic phase was dried with MgSO₄, filtered, and the solvent evaporated in vacuo. Purification by column chromatography (SiO₂, CH₂Cl₂/hexane 7:3 v/v, $R_f = 0.51$) yielded **14** (2.42 g, 70%) as a light yellow solid. Mp 65–66 °C. ^1H NMR (300 MHz, CDCl₃): $\delta = 7.90$ (s, 2 H), 2.51 (s, 6 H), 0.29 (s, 9 H) ppm. ^{13}C NMR (75 MHz, CDCl₃): $\delta = 146.6$, 142.4, 130.0, 121.6, 109.2, 101.0, 21.4, 0.1 ppm. Calcd for C₁₃H₁₇NO₂Si (247.37): C 63.12, H 6.93, N 5.66; found: C 63.11, H 6.96, N 5.59%. MS (ESP+): $m/z = 248.0$ [MH⁺].

3,5-Dimethyl-4-(triisopropylsilylethynyl)nitrobenzene (15).

The idonitrobenzene **11** (4.92 g, 17.8 mmol) was dissolved in dry, degassed THF (60 mL) under an argon atmosphere. Diisopropylamine (10 mL), CuI (16 mg, 0.084 mmol), and [PdCl₂(PPh₃)₂] (400 mg, 0.570 mmol) were added, and the solution was degassed by sonication under argon atmosphere for 20 min. Then triisopropylsilylacetylene (8.0 mL, 36 mmol) was added, and the solution was stirred at 45–50 °C for 2 days. The solution was diluted with Et₂O (200 mL) and washed with saturated aqueous NH₄Cl (2 × 150 mL). The organic phase was dried with MgSO₄, filtered, and the solvent evaporated in vacuo. Purification by column chromatography (SiO₂, toluene/heptanes 3:7 v/v, $R_f = 0.52$) yielded **15** (4.27 g, 72%) as a light yellow solid (and **16** as byproduct as a yellow powder, 0.55 g,

10%). Mp 49–50 °C. ^1H NMR (300 MHz, CDCl_3): δ = 7.92 (s, 2 H), 2.54 (s, 6 H), 1.16 (s, 21 H) ppm. ^{13}C NMR (75 MHz, CDCl_3 , delay = 1.5 s, acquisition time = 3.4 s): δ = 146.5, 142.4, 130.4, 121.7, 106.1, 102.8, 21.7, 18.9, 11.5 ppm. Calcd for $\text{C}_{19}\text{H}_{29}\text{NO}_2\text{Si}$ (331.52): C 68.83, H 8.82, N 4.22; found: C 68.89, H 8.94, N 4.22%. MS (ESP+): m/z = 332.2 [MH^+].

1,2-Bis(3,5-dimethyl-4-((triisopropylsilyl)ethynyl)phenyl)diazene oxide (16) (byproduct). Yellow powder. Mp 156.0–156.5 °C. ^1H NMR (300 MHz, CDCl_3): δ = 7.98 (s, 2 H), 7.90 (s, 2 H), 2.55 (s, 6 H), 2.52 (s, 6 H), 1.17 (s, 21 H), 1.16 (s, 21 H) ppm. ^{13}C NMR (75 MHz, CDCl_3): δ = 147.0, 143.2, 141.9, 141.3, 127.2, 125.1, 123.9, 120.6, 104.6, 103.6, 103.4, 102.0, 21.8, 21.7, 19.0, 19.0, 11.6, 11.6 ppm. Calcd for $\text{C}_{38}\text{H}_{58}\text{N}_2\text{OSi}_2$ (615.05): C 74.21, H 9.50, N 4.55; found: C 74.09, H 9.62, N 4.48%. MS (ESP+): m/z = 615.4 [MH^+]. IR (KBr): 3436s, 2864s, 2890s, 2964s, 2942s, 2146m, 1469s ($N = \text{NO}$) cm^{-1} .

3,5-Dimethyl-4-ethynylaniline (18). Compound **13** (600 mg, 2.76 mmol) was dissolved in THF (10 mL). MeOH (10 mL) and K_2CO_3 (546 mg, 5.52 mmol) were added, and the mixture was stirred at rt overnight. The reaction mixture was diluted with Et_2O (50 mL), washed with saturated aqueous NH_4Cl (2 \times 50 mL), dried with MgSO_4 and the solvent evaporated in vacuo. Purification by column chromatography (SiO_2 , EtOAc /heptanes 1:1 v/v, R_f = 0.50) yielded **18** (228 mg, 57%) as an orange solid. Mp 71.5–73.0 °C. ^1H NMR (300 MHz, CDCl_3): δ = 6.36 (s, 2 H), 3.67 (br s, 2 H), 3.38 (s, 1 H), 2.36 (s, 6 H) ppm. ^{13}C NMR (75 MHz, CDCl_3): δ = 146.5, 142.7, 113.5, 112.0, 83.1, 82.1, 21.3 ppm. Calcd for $\text{C}_{10}\text{H}_{11}\text{N}$ (145.20): C 82.72, H 7.64, N 9.65; found: C 82.62, H 7.82, N 9.64. MS (ESP+): m/z = 146.1 [MH^+].

3,5-Dimethyl-4-ethynynitrobenzene (19). Compound **15** (1.27 g, 3.83 mmol) was dissolved in wet THF (20 mL). A solution of tetrabutylammonium fluoride in THF (1 mL, 1 mmol, 1 M) was added and the solution was stirred for 10 min at rt. Water was added to the solution until it became colorless. The reaction mixture was diluted with Et_2O (100 mL), washed with saturated aqueous NH_4Cl (2 \times 100 mL), dried with MgSO_4 and the solvent evaporated in vacuo. Purification by column chromatography (SiO_2 , CH_2Cl_2 /heptanes 4:6 v/v, R_f = 0.55) yielded **19** (610 mg, 91%) as a colorless solid. Mp 170 °C. ^1H NMR (300 MHz, CDCl_3): δ = 7.92 (s, 2 H), 3.78 (s, 1 H), 2.54 (s, 6 H) ppm. ^{13}C NMR (75 MHz, CDCl_3): δ = 147.0, 142.9, 128.9, 121.7, 90.5, 79.8, 21.4 ppm. Calcd for $\text{C}_{10}\text{H}_9\text{NO}_2$ (175.18): C 68.56, H 5.18, N 8.00; found: C 68.18, H 5.13, N 7.83%. MS (ESP+): m/z = 176.1 [MH^+].

7-[(2,6-Dimethylphenyl)ethynyl]-2-phenyl-1,8a-dihydroazulene-1,1-dicarbonitrile (20a). A crude batch of **2a**, synthesized from 7,8-dibromo-2-phenyl-1,7,8,8a-tetrahydroazulene-1,1-dicarbonitrile (416 mg, 1.00 mmol), and the terminal acetylene **17** (260 mg, 2.00 mmol) were dissolved in dry, degassed THF (10 mL) under argon atmosphere. Diisopropylamine (0.5 mL), CuI (3.8 mg, 0.020 mmol), and $[\text{PdCl}_2(\text{PPh}_3)_2]$ (70 mg, 0.10 mmol) were added, and the solution was subjected to sonication under argon atmosphere for 2 h at 40 °C. The reaction mixture was concentrated in vacuo. Purification by column chromatography (SiO_2 , toluene, R_f = 0.55) yielded **20a** (138 mg, 36%) as a yellow solid or foam. Mp 170.0–171.5 °C. ^1H NMR (300 MHz, CDCl_3): δ = 7.73–7.76 (m, 2 H), 7.43–7.51 (m, 3 H), 7.10–7.14 (m, 1 H), 7.02–7.07 (m, 2 H), 6.91 (s, 1 H), 6.62–6.63 (m, 2 H), 6.32 (d, 3J = 5.2 Hz, 1 H), 6.20 (d, 3J = 4.6 Hz, 1 H), 3.88 (dd, 3J = 4.6 Hz, 4J = 1.7 Hz, 1 H), 2.45 (s, 6 H) ppm. ^{13}C NMR (75 MHz, CDCl_3): δ = 141.3, 140.6, 140.5, 132.6, 131.9, 131.5, 130.5, 129.5, 128.3, 126.9, 126.6, 123.8, 123.5, 122.6, 120.7, 115.1, 112.8, 96.2, 87.5, 51.1, 45.1, 21.3 ppm; one signal missing. Calcd for $\text{C}_{28}\text{H}_{20}\text{N}_2$ (384.47): C 87.47, H 5.24, N 7.29; found: C 87.38, H 5.33, N 7.00%.

7-[(4-Amino-2,6-dimethylphenyl)ethynyl]-2-phenyl-1,8a-dihydroazulene-1,1-dicarbonitrile (21a). A crude batch of **2a**, synthesized from 7,8-dibromo-2-phenyl-1,7,8,8a-tetrahydroazulene-1,1-dicarbonitrile (208 mg, 0.50 mmol), and the terminal acetylene **17** (290.4 mg, 1.00 mmol) were dissolved in dry,

degassed THF (10 mL) under argon atmosphere. Diisopropylamine (0.5 mL), CuI (1.9 mg, 0.01 mmol), and $[\text{PdCl}_2(\text{PPh}_3)_2]$ (35 mg, 0.05 mmol) were added, and the solution was subjected to sonication under argon atmosphere for 3 h at 40 °C. The reaction mixture was concentrated in vacuo. Purification by column chromatography (SiO_2 , CH_2Cl_2 , R_f = 0.30) yielded **20a** (200 mg, 50%) as a yellow to brown solid. ^1H NMR (300 MHz, CDCl_3): δ = 7.74–7.77 (m, 2 H), 7.44–7.52 (m, 3 H), 6.89 (s, 1 H), 6.61 (d, 3J = 3.4 Hz, 2 H), 6.37 (s, 2 H), 6.33 (m, 1 H), 6.14 (d, 3J = 4.6 Hz, 1 H), 3.88 (dd, 3J = 4.6 Hz, 4J = 1.7 Hz, 1 H), 3.69 (br s, 1 H), 2.36 (s, 6 H) ppm. ^{13}C NMR (75 MHz, CDCl_3): δ = 146.6; 142.3; 141.2; 140.6; 133.0; 132.0; 131.2; 130.6; 130.4; 129.5; 126.6; 124.0; 122.6; 120.7; 115.2; 113.6; 112.8; 112.5; 94.1; 88.5; 51.2; 45.2; 21.4 ppm. HR-MS (ESP+): m/z = 422.1629 [MNa^+]; calcd for $\text{C}_{26}\text{H}_{21}\text{N}_3\text{Na}$: m/z = 422.1633.

7-[(4-Nitro-2,6-dimethylphenyl)ethynyl]-2-phenyl-1,8a-dihydroazulene-1,1-dicarbonitrile (22a). Method 1. A crude batch of **2a**, synthesized from 7,8-dibromo-2-phenyl-1,7,8,8a-tetrahydroazulene-1,1-dicarbonitrile (208 mg, 0.50 mmol), and the terminal acetylene **19** (175 mg, 1.00 mmol) were dissolved in dry, degassed THF (5 mL) under argon atmosphere. Diisopropylamine (0.20 mL), CuI (1.9 mg, 0.010 mmol) and $[\text{PdCl}_2(\text{PPh}_3)_2]$ (35.1 mg, 0.05 mmol) were added, and the solution was subjected to sonication under argon atmosphere for 7 h at 40 °C. The reaction mixture was concentrated in vacuo. Purification by column chromatography (SiO_2 , toluene, R_f = 0.56) yielded **22a** (43 mg, 20%) as a yellow solid or foam.

Method 2. The ethynyl-DHA **6a** (70 mg, 0.25 mmol) was dissolved in dry degassed THF (5 mL) under argon atmosphere. 3,5-Dimethyl-4-iodonitrobenzene **11** (277 mg, 1.00 mmol), $[\text{Pd}(\text{PPh}_3)_4]$ (17.5 mg, 0.025 mmol), CuI (0.9 mg, 0.005 mmol), and diisopropylamine (0.1 mL) were added, and the solution was stirred for 2 h at 40 °C. The reaction mixture was concentrated in vacuo. Purification by column chromatography (SiO_2 , toluene, R_f = 0.56) yielded **22a** (17 mg, 17%) as a yellow solid or foam. ^1H NMR (300 MHz, CDCl_3): δ = 7.93 (s, 1 H), 7.75–7.78 (m, 2 H), 7.42–7.53 (m, 3 H), 6.93 (s, 1 H), 6.59–6.73 (m, 2 H), 6.38 (d, 3J = 5.9 Hz, 1 H), 6.27 (d, 3J = 4.7 Hz, 1 H), 3.90 (dd, 3J = 4.7 Hz, 4J = 1.7 Hz, 1H), 2.54 (s, 6 H) ppm. ^{13}C NMR (75 MHz, CDCl_3): δ = 146.8; 142.1; 141.7; 140.6; 132.2; 131.8; 131.7; 130.7; 130.3; 129.6; 129.5; 126.6; 125.3; 122.7; 121.7; 120.7; 115.0; 112.8; 101.0; 85.8; 51.2; 45.1; 21.5 ppm. HR-MS (ESP+): m/z = 452.1386 [MNa^+]; calcd for $\text{C}_{28}\text{H}_{19}\text{N}_3\text{O}_2\text{Na}$: m/z = 452.1375.

Crystallographic Details of Compound 16. Data were recorded on a Nonius KappaCCD diffractometer using MoK_α radiation with a graphite monochromator. Data reduction was performed with EvalCCD.²² The structure was determined and refined with SHELXS and SHELXL, respectively,^{23,24} as implemented in maXus.²⁵ The isopropyl groups attached to the silicon atoms display both static and dynamic disorder. One of the isopropyl groups are described with two conformations almost equally populated (0.54:0.46). The independent isopropyl groups were restrained to be structurally alike (SHELXL97 SADI instructions). Also the SHELXL97 SIMU (restraining to isotropic temperature parameters) and DELU (alike anisotropic parameters for bonded atoms) instructions were applied to restrain the refinement. Thermal ellipsoid plots were made with ORTEP²⁶ as implemented in the program PLATON.²⁷ The CIF-file was checked with PLATON and the program enCIFer from the

(22) Duisenberg, A. J. M.; Kroon-Batenburg, L. M. J.; Schreurs, A. M. M. *J. Appl. Crystallogr.* **2003**, *36*, 220–229.

(23) Sheldrick, G. M. *Acta Crystallogr. A* **1990**, *46*, 467–473.

(24) Sheldrick, G. M. *SHELXL97, Program for the refinement of crystal structures*; University of Göttingen: Germany, 1997.

(25) Mackay, S.; Gilmore, C. J.; Edwards, C.; Stewart, N.; Shankland, K. 1999. *maXus Computer program for the solution and refinement of crystal structures*; Bruker Nonius: The Netherlands, 1999.

(26) Johnson, C. K. *ORTEP-II, A Fortran thermal-ellipsoid plot program. Report ORNL-5138*; Oak Ridge National Laboratory: Oak Ridge, TN, 1976.

(27) Spek, A. L. *PLATON, A Multipurpose Crystallographic Tool*; Utrecht University: Utrecht, The Netherlands, 2001.

Cambridge Crystallographic Data Centre (www.ccdc.cam.ac.uk), from where the structure is available on demand with accession code CCDC771508.

Acknowledgment. The Danish Research Council for Independent Research | Natural Sciences is gratefully acknowledged for financial support. In addition, the research leading to these results has received funding from the European Community's Seventh Framework Programme (FP7/2007-2013) under the grant agreement "SINGLE" no 213609.

Supporting Information Available: NMR spectra, UV–vis spectra showing the photo- and thermal switching events, Arrhenius plots for the ring-closure reaction, complete ref 18, computational data, and X-ray data. This material is available free of charge via the Internet at <http://pubs.acs.org>.

JA103235G